Lithofacies Characterization in Seismic Space Using Rock Physics-based Decoupling: Application to Niger Delta Turbidite Reservoirs

Olatunbosun Olagundoye[1], Sunday Amoyedo[1], Loreline Kaucsar[2], Eric Tawile[2], and Christopher Enuma[1]
[1]TotalEnergies, Lagos, Nigeria [2]TotalEnergies, Pau, France

ABSTRACT

Lithofacies characterization is commonly used in reservoir model building, well planning and placement, and reservoir management because facies majorly control porosity and permeability. However, lithofacies characterization or classification in seismic space is highly dependent on the ability to relate lithofacies to significant variations in rock physics, and seismic properties. The complex nature of turbidites, linked principally to their heterogeneous nature arising from successive sedimentation, erosional episodes, and tectonics, usually complicates this dependency due to significant overlaps in rock physics behavior among lithofacies in different stratigraphic intervals in the same producing field. These overlaps often bias lithofacies classification in turbidite reservoirs if rock physics-based reservoir decoupling is not applied. To show how this bias and the resultant uncertainties in the predictiveness of facies probability cubes can be avoided, we present a case study from an oil field in the Deep Offshore Niger Delta, which comprises of Middle to Late Miocene sands and shales. The reservoirs are in a highly faulted turbidite setting within a framework consisting of seven grouped electrofacies. Multi-well rock physics analysis at seismic scale was applied to identify statistical facies populations that exhibit significant overlaps in rock physics properties across stratigraphic intervals. Based on facies overlap sensitivities in rock physics space using inverted IP and Vp/Vs attributes from Ocean Bottom Nodes (OBN) seismic data extracted at training wells, the vertical sequence was divided into three separate intervals consisting of facies with seismically important rock physics variations. Facies probability cubes produced using the decoupling approach exhibited better correlations at wells, in comparison to those produced using the conventional technique. Cross validation at blind wells indicated that the decoupled facies cubes are more predictive. Additional QCs showed that the facies cubes are robust as input for reservoir model building, well design and placement, and reservoir management.

Keywords: Lithofacies, Turbidites, Seismic Attributes, Inversion, Ocean Bottom Nodes (OBN), Rock Physics.

INTRODUCTION

Seismic reservoir characterization consists of strategies and quantitative seismic interpretation techniques such as AVO/AVA analysis, seismic inversion, seismic attribute analysis, lithofacies (lithology and fluids) characterization or classification, et cetera applied in hydrocarbon exploration and/or development for the description of reservoir units relative to their bounding materials (i.e., non-reservoirs). Abundant literature exists on the definitions, theory, and applications of seismic reservoir characterization (Hunt *et. al.,* 2012; Avseth *et. al.,* 2014; Oliveira *et al.,* 2018). Over the years, declining oil revenues have tilted business models in the oil industry towards cost efficient recovery optimization from existing fields and the targeting of nearby undeveloped prospects or infills to enhance productivity and investment returns. Like other petroliferous basins, seismic reservoir characterization is routinely applied in oil fields in the Niger Delta in reservoir model building, well placement, reservoir monitoring, the targeting of infills or undeveloped hydrocarbon pools, which may either be laterally or vertically offset from developed areas of both green and brown fields.

This paper highlights the application of lithofacies characterization in seismic space (i.e., a quantitative seismic interpretation technique) to provide lithofacies probability volumes from inverted Ocean Bottom Nodes (OBN) seismic data in a turbidite oil field in the deep offshore Niger Delta. The lithofacies volumes were required to provide quantitative information on the distribution of geological facies, porosities, and permeabilities for reservoir model building, well planning, geosteering, and reservoir management.

© Copyright 2021. Nigerian Association of Petroleum Explorationists.
All rights reserved.

This research was financed by the Petroleum Technology Development Fund (PTDF) scholarship. The research also benefitted from discussions with the Academic Board of the Department of Geology and Prof. A. U. Okoro. Special thanks go to Chidubem O. Emedo for his immense help during the fieldwork. Anonymous reviews of the manuscript are also acknowledged.

Lithologies in the study area consists of shales and sands which are heterogeneous due to a deep water setting which in geologic past was conducive for successive sedimentation, erosional episodes, and tectonics. Lithofacies characterization is the seismic classification of petrophysical properties or lithofacies based on the availability of a robust link between cross plot-based rock physics behavior (e.g., acoustic impedance, IP versus Vp/Vs color coded by volume of clay) and the reservoir property (e.g., volume of clay) of the lithofacies of interest. Being a classification in seismic space, it is highly dependent on the ability to relate lithofacies to significant variations in rock physics, and indeed seismic properties. To say the least, the complex nature of turbidites, linked principally to their heterogeneous geologic nature may sometimes complicate the seismic space lithofacies classification due to significant overlaps in rock physics behavior among lithofacies in different stratigraphic intervals in the same producing field. These overlaps often bias lithofacies classification in turbidite reservoirs with resultant uncertainties in the predictiveness of facies probability if rock physics-based reservoir (interval) decoupling is not applied. Figure 1 provides a simple illustration of the principle of lithofacies probability characterization or estimations from a rock physics attribute cross plot. According to Michelena *et. al.,* (2010), a rectangular grid is superimposed on the cross plot and individual probabilities of the different scenarios (red and blue dots) are calculated for each rectangle, with probabilities then assigned throughout the whole 3D seismic volume. Further analysis of the cross plot reveals two major regions of overlap between the red "facies" and blue "facies" which correlate with higher and lower probabilities of red "facies". Statistically, it would be easier to characterize the blue "facies" in the region with lower probability of red "facies" due to the much lower overlap. The reverse is however not the case in the region with higher probability of red "facies". This reverse case is the scenario that the current study handles in our study area.

Some authors have recognized that lithofacies characterization works best when there is no significant overlap in rock physics behavior between lithofacies and have proposed some quantitative statistical schemes (e.g., facies flagging based colored multi-dimensional cross-plotting, geostatistical inversion, et cetera) to overcome this limitation in seismic (i.e., elastic) space (Michelena *et. al.,* 2010; Pendrel *et. al.,* 2017; Singh *et. al.,* 2019). However, these approaches are to a certain degree computationally intensive and require various assumptions. In this study, we apply a qualitative based decoupling approach which entails the separation of a gross logged interval into distinct sub-intervals whose lithofacies do not suffer significant overlap in rock

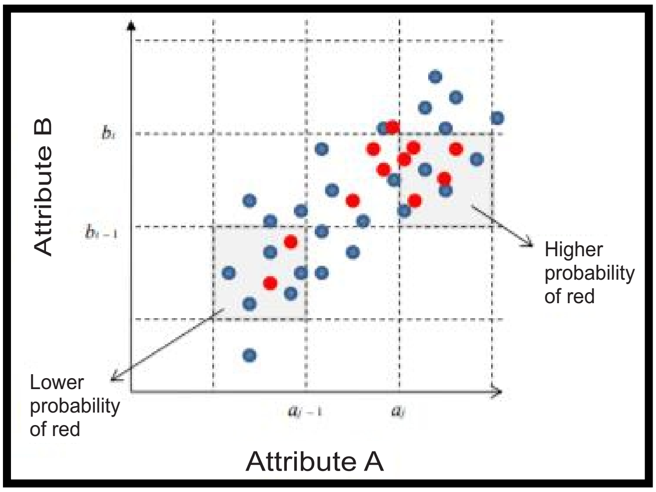

Figure 1: Probability estimations from attribute cross plots illustrating the principle of lithofacies characterization. A rectangular grid is superimposed on the cross plot and individual probabilities of the different scenarios (red and blue dots or facies) are calculated for each rectangle. These probabilities are then assigned throughout the whole seismic volume. After Michelena *et. al.,* (2010).

physics behavior. To avoid uncertainties in the predictiveness of facies probability cubes due to observed overlaps in rock physics behavior among lithofacies in the study area, multi-well rock physics analysis at seismic scale was applied in this study to identify statistical facies populations that exhibit significant overlaps in rock physics properties across stratigraphic intervals. Based on facies overlap sensitivities in rock physics space using inverted IP and VP/Vs attributes from the inverted OBN seismic data extracted at training wells, the vertical sequence was divided into three separate intervals consisting of facies with seismically distinguishable rock physics variations. Facies probability cubes produced using the decoupling approach exhibited better correlations at wells, in comparison to those produced using the conventional technique. Cross validation at blind wells indicated that the decoupled facies cubes are more predictive. Additional QCs at training wells and attribute extractions showed that the facies cubes are robust enough for reservoir modeling, well design & placement, and reservoir management.

Location and Geology

The study area (pseudo named Delta Field) lies in an Oil Mining Lease (OML) in the deep offshore Niger Delta (Figure 2). The Niger delta basin is situated in the Gulf of Guinea and extends throughout the Niger delta Province (Klett *et al.,* 1997). According to Tuttle *et al.* (1999), the delta formed at the site of a rift triple junction related to the opening of the southern Atlantic starting in the Late

Jurassic and continuing into the Cretaceous. They further stated that one petroleum system called the Tertiary Niger Delta (Akata-Agbada) petroleum system has been identified in the basin, and that oil and gas resources are more than 35 billion barrels of recoverable oil and 90 trillion cubic feet of recoverable gas. The geology of the Niger delta has been documented by several authors (Short and Stauble, 1965; Weber and Daukoru, 1975; Weber, 1987; Ekweozor and Daukoru, 1994; Reijers *et al.,* 1997). Figure 2 illustrates the tectonic division of the delta into three distinct zones (i.e., upper extensional, transitional, and lower compressional), the conceptual depositional model of the Delta Field, and its location in the transitional zone (Central Plateau) which is very complex and characterized by faults, toe-thrusts, diapiric and shale ridges.

Structurally, the field exists within a NE-SW trending dual-culmination anticline. The field is characterized by a complex reservoir system which consists of multi-layered reservoirs in Miocene turbidites complexes in several stratigraphic sequences (mainly sands, shales, and debris flows) within a burial range of 1100 m and 1700 m. The main reservoir intervals are the R12, R18, and R24 (i.e., regarded as Intervals 1, 2, and 3 in this study; Figure 3). A random seismic line in Figure 3 shows the main reservoir intervals based on the correlation between six (6) key wells in the field. The thickness of sands in the R18 interval varies between 25 and 63 meters, while that of the R24 and R12 varies between 30 and 56 meters and 4 to 21 meters respectively. In terms of petrophysical properties, the reservoir intervals in the field have porosities ranging from 17% to 25%.

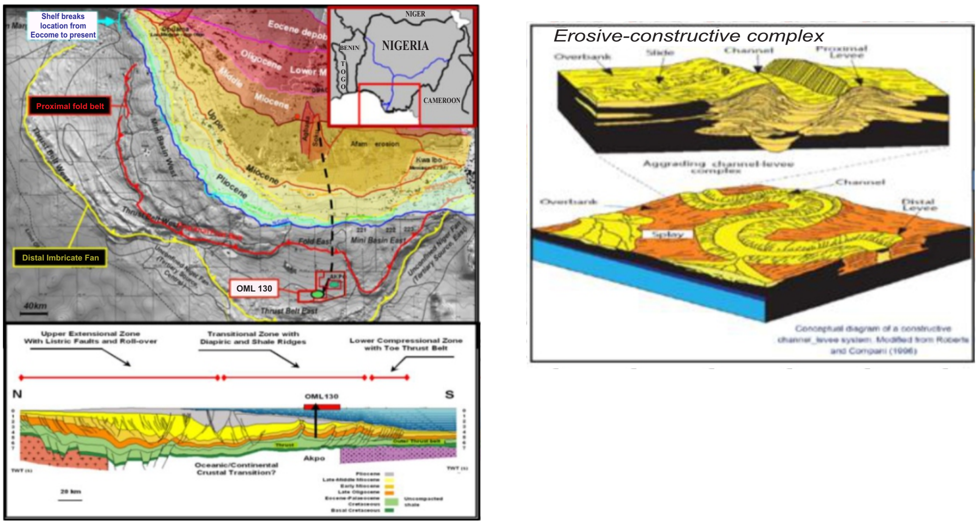

Figure 2: Location of study area (Delta Field), Deep Offshore, Niger Delta.

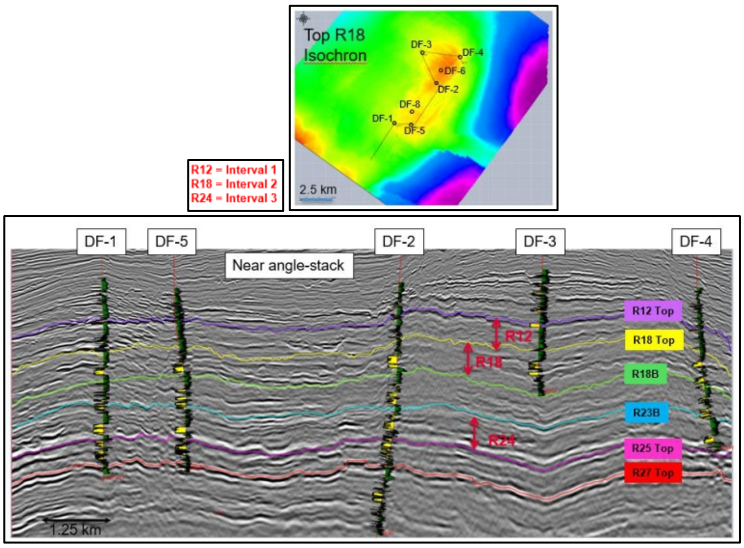

Figure 3: Main reservoir intervals in the study area (Delta Field) based on the correlation between 5 wells using Ocean Bottom Nodes (OBN) seismic data. Note the heterogeneous seismic character which highlight variability or heterogeneity in seismic properties. Wells DF-1, 2, 3, 4, 5, and 8 on the isochron represent the wells used as learning / training data during the lithofacies characterization, with DF-6 serving as the blind well.

DATA

Three main datasets were used in this study: namely logs, lithofacies, and seismic data. The conventional log data set consisted of environmentally corrected and edited versions of gamma ray, resistivity, full-wave sonic (compressional and shear), neutron-density, PEF (photoelectric factor), and quantitative volume of clay (Vcl) log data from 7 wells (DF-1, DF-2, DF-3, DF-4, DF-5, DF6, and DF-8; Figure 3). Multivariate statistics and regression-based electrofacies (EFs) derived from sets of well log responses that are unique to facies served as the lithofacies dataset for the 7 wells. Wells DF-1, DF-2, DF-3, DF-4, DF-5, and DF-6 were used as training wells, while well DF-8 was used as blind well.

On the other hand, the seismic data was mainly made up of inverted IP (acoustic impedance) and Vp/Vs (P-velocity/S-velocity) elastic attributes from Ocean Bottom Nodes (OBN) 3D seismic data. Other data included horizons (isochrons) and faults that were interpreted from the seismic data. The isochron map in Figure 3 shows the areal coverage of the inverted seismic data. The Delta field is covered by both streamer and OBN 3D seismic data acquisition vintages acquired in 2016 and 2019 respectively (Figure 4). These two seismic vintages represent efforts to resolve structural, stratigraphic, and reservoir monitoring challenges in the field (such as fault shadowing, resolution, repeatability, etc.). High seismic energy loss in the reservoir intervals due to overburden complexities (e.g., shallow gas effects, mud volcanoes, and shallow turbidite fairways) necessitated the acquisition of the OBN seismic survey. The seismic energy loss is quite problematic in the earlier seismic vintage (i.e., 3D streamer; Figure 4), leading to 3D seismic inversion results not being sufficiently optimal for seismic reservoir characterization.

Currently, the OBN seismic data serves as the reference vintage in the study area for qualitative and quantitative seismic interpretation due to improved imaging and its intended use as a baseline for 4D seismic reservoir monitoring. Chakraborty (2017) regards the OBN seismic data acquisition technique as optimum for reservoir characterization due to its characteristic long offset, full azimuth data and high-quality low frequency content. Seismic inversion attributes (IP and Vp/Vs) from the OBN seismic data were chosen (in preference to those from the streamer vintage) as seismic input for the lithofacies characterization due to better energy penetration at the reservoir level (from long offset coverage and post stack AVO-consistent amplitude normalization), a robust velocity field, high-quality low frequency content and improved signal to noise ratio (SNR). The spectral comparison of the older streamer and OBN seismic data in Figure 5 highlights the improvement

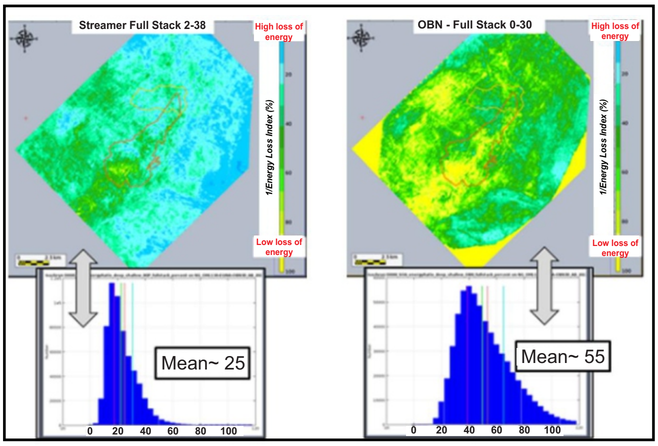

Figure 4: Inverse of energy loss index estimations (%) for Streamer (left) versus OBN (right) highlighting the seismic energy preservation in interval 2 (R12) of the Delta Field. Modified after Amoyedo *et. al.,* (2020).

in frequency bandwidth and higher SNR in the OBN data. In addition, our choice of the inverted OBN seismic data was supported by better seismic characterization derived from it when compared to the streamer vintage elastic inversion. Amoyedo *et. al.,* (2020) and Tawile *et al.,* (2020) noted that the ratio of P-velocity to S-velocity (Vp/Vs) from the inverted OBN data which is a good indicator of sandy reservoirs in the study area, matched well results much better than the vintage streamer data (6). Their observations are further supported by quantitative estimates of correlation using the probability of success (POS) in volume of clay (Vcl) prediction at the two wells (DF-1 and DF-2) in Figure 6, which are based on comparisons between well log Vcl and OBN inversion predicted (i.e., pseudo) Vcl in relation to those from the older streamer inversion data. The POS from the OBN inversion seismic data range for the DF-1 and DF-2 wells were 74% and 83% relative to 44% and 70% from the narrow azimuth streamer inversion data. These POS values highlight the high quality of the OBN inversion (and well data) for lithofacies characterization.

METHODOLOGY

Lithofacies characterization in seismic space aimed at obtaining volumes of the probability of lithofacies in 3D geologic space, entails the determination of probability density functions (PDFs) or operators for each lithofacies at wells from 3D seismic data (e.g., inverted seismic attributes or elastic inversions) and subsequent application of these operators or PDFs in a convolutional manner to the 3D seismic data. The quality of the characterization is dependent on adequate data QCs (such as well log data checks and validations, robust seismic-to-well calibrations, and inverted attribute QCs) and the existence of rock physics behaviors that can be directly to

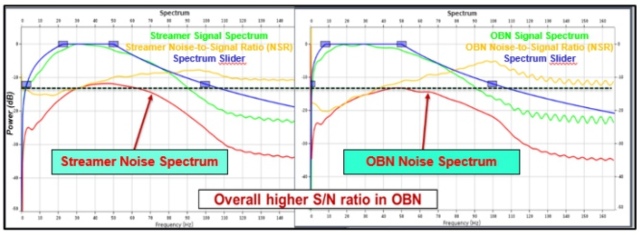

Figure 5: Power spectral comparison between Streamer and OBN seismic data. Note the improved frequency bandwidth (at cut-offs of -6dB and -12dB) and lower noise content in the OBN seismic frequency spectrum. Modified from Amoyedo *et. al.,* (2020).

overlap in inverted attributes cross-plots (e.g., IP versus Vp/Vs color coded by GEFs). This analysis is critical to determine if lithofacies characterization would be viable in the study area, and that the inverted IP and Vp/Vs attributes are suitable for the discrimination of lithofacies. Also, analysis of the lithofacies overlaps in the cross plots give insights into the need for merging of lithofacies or GEFs based on similarities in rock physics behavior. The second step is directed at merging of lithofacies or GEFs using clustering analysis in rock physics space at seismic scale. GEFs or lithofacies are merged when significant overlap exists in rock physics behavior between them. Continuous PDFs for each lithofacies are then built from

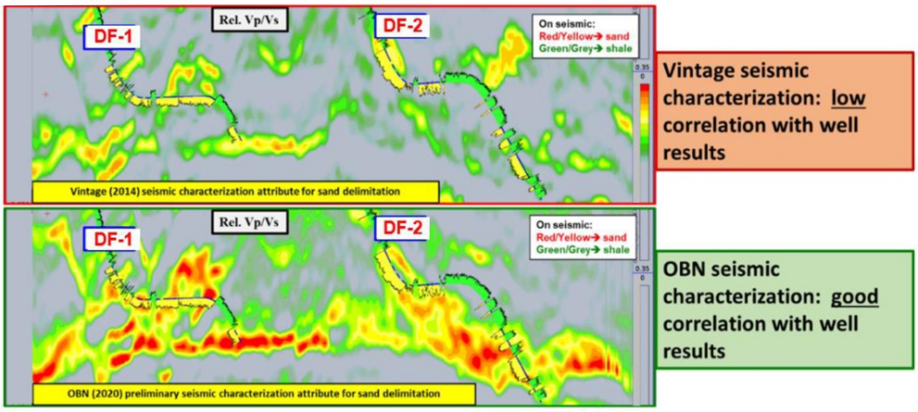

Figure 6: Comparison of seismic reservoir characterization quality between streamer inverted Vp/Vs (top section) and OBN inverted Vp/Vs (bottom section). Note the improved sand/shale characterization and much better correlation with well results from the OBN-derived Vp/Vs. Modified after Amoyedo et. al., (2020) and Tawile *et. al.,* (2020).

lithofacies. In this study, our focus was mainly directed towards the rock physics aspect. Moreover, aspects of the QCs of our datasets have already been detailed in the data section of this paper, and in literatures published by Amoyedo et al., (2020) and Tawile *et. al.,* (2020).

To perform the lithofacies classification in seismic space, our methodology involved incorporating an additional step (which we term reservoir or interval decoupling) into the traditional classification workflow (Figure 7). Based on the assumption that all input datasets (i.e., well data and extracted seismic attributes) are optimum (i.e., positive results from relevant QCs such as log data checks and validations, robust seismic-to-well calibrations, and inverted attribute QCs), the workflow for lithofacies classification traditionally involves: first, determining the seismic scale dependence or sensitivity of upscaled lithofacies (i.e., Grouped Electro-facies, GEFs in this study) in the study area to the inverted attributes (IP and Vp/Vs) of the OBN seismic data. The lithofacies upscaling is achieved by resampling merged GEFs to the same time sampling interval of the inverted attributes (i.e., 3 milliseconds in our case). The sensitivity analysis is necessary to determine which lithofacies can be discriminated in seismic space based on the degree of discrete set of points in the IP versus Vp/Vs cross-plot after the second step. Finally, the operators or PDFs are applied in the full 3D volume based on a convolution process to obtain the probability (%) of each of the lithofacies in the input 3D seismic grid.

However, the complex nature of turbidites usually complicates the traditional characterization process or workflow due to significant overlaps in rock physics behavior of lithofacies. These overlaps result in biases and uncertainties in the predictiveness of facies probability cubes (Figure 1), leading to poor input data for reservoir modeling, well optimization (i.e., planning and placement), and reservoir management. Importantly, lithofacies characterization in gas/oil fields is dependent on the discriminative rock physics behavior(s) of lithofacies. In our view, this requirement is a standard in seismic reservoir characterization. This point is underscored by Dodd *et. al.,* (2007) who opine that a sound rock physics basis is required for understanding factors controlling subsurface geophysical responses acquired from data such as seismic, wireline logs, and vertical seismic profiles (VSPs).

Generally, lithofacies possesses distinct rock physics

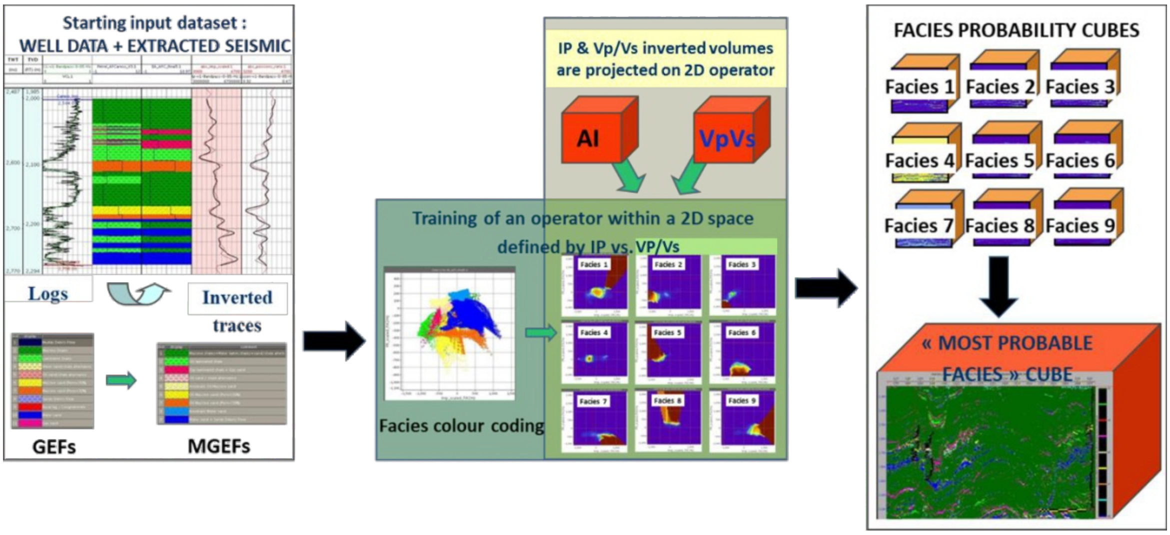

Figure 7: Typical lithofacies classification workflow for translating 3D elastic inversion outputs to facies probability cubes.

behavior which can be used to discriminate or distinguish it from others (Figure 1). Based on significant overlaps between some lithofacies across different producing turbidite intervals in the Delta Field, we therefore designed an additional step of seismic scale dependency or sensitivity analysis to avoid biases and uncertainties in the predictiveness of facies probability cubes. However, this step was performed on the merged GEFs obtained from clustering analysis in rock physics space (i.e., before Step 2 of the classical characterization workflow). Primarily, this involved separating or decoupling reservoir and non-reservoir lithofacies found in multiple channel complexes that make up the gross logged interval in the Delta Field before the merging of the GEFs. Multi-well rock physics analysis at seismic scale was applied to identify statistical facies populations that exhibit significant overlaps in rock physics properties across stratigraphic intervals. Based on the facies overlap sensitivities in rock physics space using inverted IP and Vp/Vs attributes from the field's Ocean Bottom Nodes (OBN) seismic data extracted at training wells, the entire gross stratigraphic sequence was then divided into three separate intervals (1, 2, and 3; Figure 3) consisting of facies with seismically important rock physics variations.

RESULTS AND DISCUSSIONS

Seismic scale sensitivities of upscaled lithofacies (Grouped Electro-facies, GEFs) to inverted attributes (IP and Vp/Vs) from OBN seismic data

Figure 8 shows the lithofacies (GEFs) obtained from eleven (11) electrofacies associations (EFAs) defined at wells using log facies and petrophysical grouping analysis. The eleven EFAs were grouped into 6 GEFs using similarities in both log character and three key petrophysical properties (i.e., Vcl, PHIT, and PHIE). The large number of EFAs and GEFs is indicative of the complex nature of turbidites in the study area which is linked principally to heterogeneities. Typically, heterogeneities cause transitional variations between turbidite GEFs in the petroelastic/rock physics domain which are expressed as overlaps in rock physics behavior that complicate lithofacies discrimination or sensitivities at seismic scale.

The seismic scale sensitivities of upscaled GEFs using a cross plot of acoustic impedance (IP) versus P velocity/S velocity (Vp/Vs) from the OBN inversion seismic data within the gross logged interval of the Delta Field is shown in Figure 9. Upscaling to seismic scale was achieved by resampling the GEFs from 0.2m to 3ms which is the same sampling interval of the inverted attributes. Globally, the cross plot shows that GEFs can be discriminated in seismic space despite the presence of some overlaps between the facies data points. Lithofacies characterization is therefore viable in the study area, and the pair of inverted attributes (IP and Vp/Vs) are suitable for the discrimination of lithofacies. Also, some overlaps in the cross plot clearly indicate the need for merging of some lithofacies or GEFs in rock physics space at seismic scale (Figures 9, 10, and 11). For instance, overlaps between GEFs that constitute non-reservoir lithofacies (e.g., GEFs 1, 2, and 6) or between those that constitute reservoir lithofacies (e.g., GEFs 3, 4, and 5) indicate that merging into mega GEFs (MGEFs) would be required. However, some overlaps are also visible between reservoir and non-reservoir lithofacies (e.g., GEFs 4 and 5 with GEF 6) which would lead to bias and uncertainties in the prediction quality of resultant facies probability cubes. The overlaps between reservoir and non-reservoir GEFs are further discussed in the reservoir facies decoupling section. The seismo-facies in Figure 8 correspond to facies that are grouped based on expected similarity in seismic scale rock physics behaviour. This grouping is confirmed by the results in Figure 9.

In Figure 9-The global discrimination between GEFs or lithofacies is quite good indicating that lithofacies characterization is viable and that the inverted attributes (IP and Vp/Vs) are suitable for the discrimination of lithofacies. Overlaps between GEFs that constitute non-reservoir lithofacies (e.g., GEFs 1, 2, and 6) or between those that constitute reservoir lithofacies (e.g., GEFs 3, 4, and 5) indicate that merging into mega GEFs (MGEFs) would be required. However, some overlaps are visible between reservoir and non-reservoir lithofacies (e.g., GEFs 4 and 5 with GEF 6) which would lead to bias and uncertainties in the predictiveness of resultant facies probability cubes. Figure 10 explains the overlaps between GEFs that constitute non-reservoir lithofacies (e.g., GEFs 1, 2, and 6) or between those that constitute reservoir lithofacies (e.g., GEFs 3, 4, and 5) indicate that merging into reservoir and non-reservoir mega GEFs (MGEFs) would be required. However, the clustering also reveals overlaps between reservoir (GEFs 3, 4, and 5) and non-reservoir lithofacies (e.g., GEFs 1, 2, and 6) which would lead to bias and uncertainties in reservoir/non-reservoir discrimination of resultant facies probability cubes.

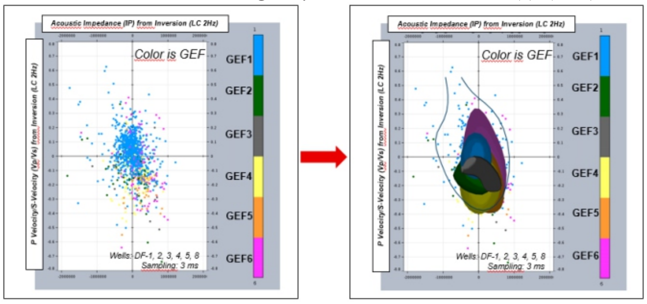

Figure 10: Overlaps of GEFs based on the clustering of dominant GEF points on cross plot of acoustic impedance (IP) versus P velocity/S velocity (Vp/Vs) from OBN inversion seismic data within gross stratigraphic interval of the Delta Field.

Electro-Facies	GEF
Organic shales	GEF 1
Hemipelagites	
Mud-turbidited LD	
Silty turbidites LD	GEF 2
Sandy turbidites LD/Alternation	
Sandy turbidites LD/No-differenciation	GEF 3
Sandy turbidites LD/Homolithic	
Fine to medium sands HD	GEF4
Medium to coarse sands HD	GEF 5
Muddy and sandy Debris-flow	GEF 6
Sandy debris-flow	

GEFs Grouping

(based on petrophysical analysis)

CLASSIFICATION			petrophysical parameters		
Interval	Seismo-facies	GEF	VCL	PHIT	PHIE
R1110 & R1120	SF 1	GEF1 GEF2	0.570	0.307	0.073
	SF 2	GEF3 GEF4 GEF5	0.092	0.338	0.300
	SF 3	GEF6	0.559	0.263	0.034
R1180E & W	SF 1	GEF1 GEF2	0.550	0.258	0.069
	SF 2	GEF3 GEF4 GEF5	0.040	0.264	0.250
	SF 3	GEF6	0.368	0.186	0.060
R1246	SF 1	GEF1 GEF2	0.548	0.183	0.038
	SF 2	GEF3 GEF4 GEF5	0.039	0.219	0.209
	SF 3	GEF6	0.390	0.137	0.033

Figure 8: Grouped Electrofacies (GEFs/Lithofacies) based on log character and petrophysical analysis of wells in the Delta Field.

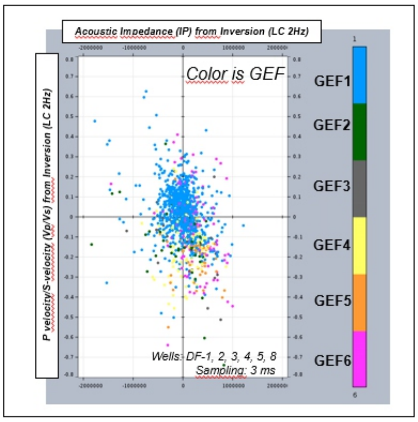

Figure 9: Seismic scale sensitivity of upscaled GEFs using cross plot of acoustic impedance (IP) versus P velocity/S velocity (Vp/Vs) from OBN inversion seismic data within gross stratigraphic interval of the Delta Field.

Multi-well rock physics-based interval decoupling

Transformation of the data points of the GEFs into clusters or polygons highlights that overlaps exist between all GEFs in the gross logged section of the wells which encompasses all the turbidite intervals in the study area (Figures 9, 10, and 11). Apart from the global overlap between all GEFs, two sub-divisions of overlaps are prominent: overlaps between individual GEFs that constitute non-reservoir lithofacies (i.e., GEFs 1, 2, and 6) or between those that constitute reservoir lithofacies (e.g., GEFs 3, 4, and 5) which indicate that merging into non-reservoir and reservoir mega GEFs (MGEFs) respectively would be required (Figures 10 and 11). The second category belongs to overlaps between reservoir lithofacies (GEFs 3, 4, and 5) and non-reservoir lithofacies (GEFs 1, 2, and 6) which would lead to bias and uncertainties in the relative reservoir/non-reservoir predictiveness of resultant facies probability cubes. Existence of this second category warrants the need for some form of decoupling to enhance the discrimination of reservoir and non-reservoir lithofacies in seismic space. This decoupling was achieved by dedicating individual cross plots to intervals within the gross logged section of the wells which show the same discriminative rock physics behavior between lithofacies (Figure 11). Generally, it is normal that different intervals within the same turbidite field may show different rock physics behavior due to differences in geologic events (i.e., sedimentation, burial history, erosional episodes, and tectonics) that affected them. These geologic events are in turn responsible for the elastic properties that drive rock physics behavior.

The cross plots show that the gross logged interval in the Delta Field can be divided into three intervals based on similarities in rock physics behavior between lithofacies (Figure 11). Qualitatively, the individual cross plot for each interval (i.e., 1, 2, and 3) displays better discrimination between GEFs compared to that of the gross logged interval. Quite importantly, the cross plots for the decoupled intervals exhibit clustered responses with much lower overlaps than the clusters on cross plot of the gross logged interval. Quantitatively, statistical facies superposition analysis results (SFSA; Figure 12) for the decoupled (i.e., 1, 2, and 3) and gross logged interval highlight a global reduction in overlaps (%) between GEFs after decoupling. Also, significant reduction in the overlaps (%) between reservoir lithofacies (GEFs 3, 4, and 5) and non-reservoir lithofacies (GEFs 1, 2, and 6) is also observable in the three separate intervals relative to the gross interval (Figure 12). These reductions provide the rock physics support for lithofacies characterization in the study area since the different lithofacies (GEFs) can now be better discriminated.

In Figure 11, the division enhances the discrimination of reservoir and non-reservoir lithofacies in seismic space by reducing the lithofacies overlaps exhibited in the gross logged interval. Primarily, this helped in decoupling reservoir lithofacies (GEFs 3, 4, and 5) from non-reservoir lithofacies (e.g., GEFs 1, 2, and 6) thus reducing uncertainties in reservoir/non-reservoir discrimination.

Merging of GEFs using clustering analysis in rock physics space at seismic scale

Some overlaps between individual GEFs that constitute non-reservoir lithofacies (i.e., GEFs 1, 2, and 6), and reservoir lithofacies (e.g., GEFs 3, 4, and 5) were still visible after the rock physics based lithofacies decoupling (Figures 11 and 12). Such overlaps indicate that it would not be possible to discriminate these facies from each other. For example, discrimination between GEFs 3, 4,

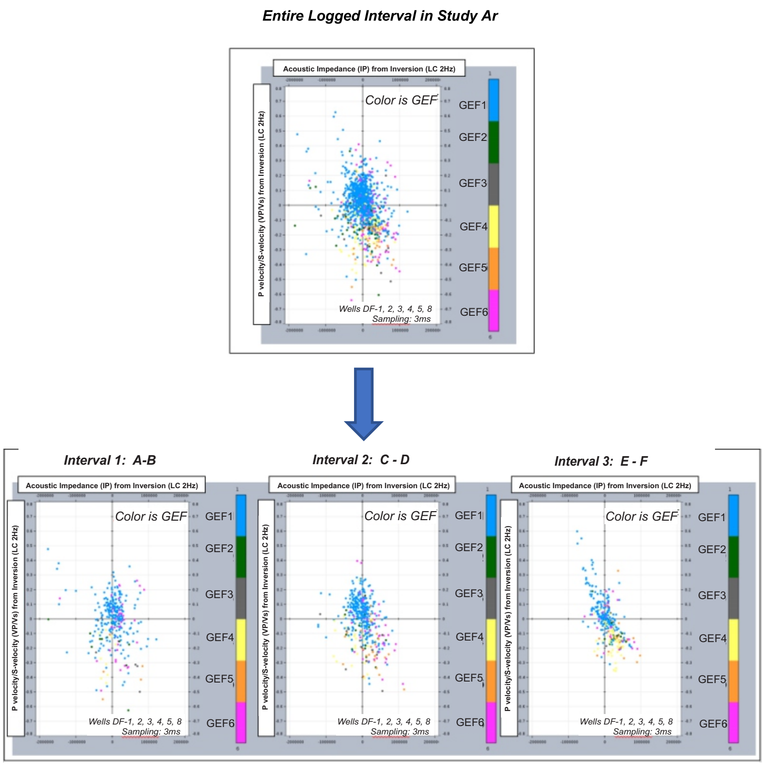

Figure 11: Division of entire logged interval of the study area into three intervals based on similarities in rock physics behavior.

and 5 would be difficult. However, GEF 6 showed minimal overlap with GEFs 1 and 2 amongst the non-reservoir lithofacies, with GEFs 1 and 2 showing large overlap. In lithofacies characterization, lithofacies which overlap in rock physics cross plots (i.e., due to similarity

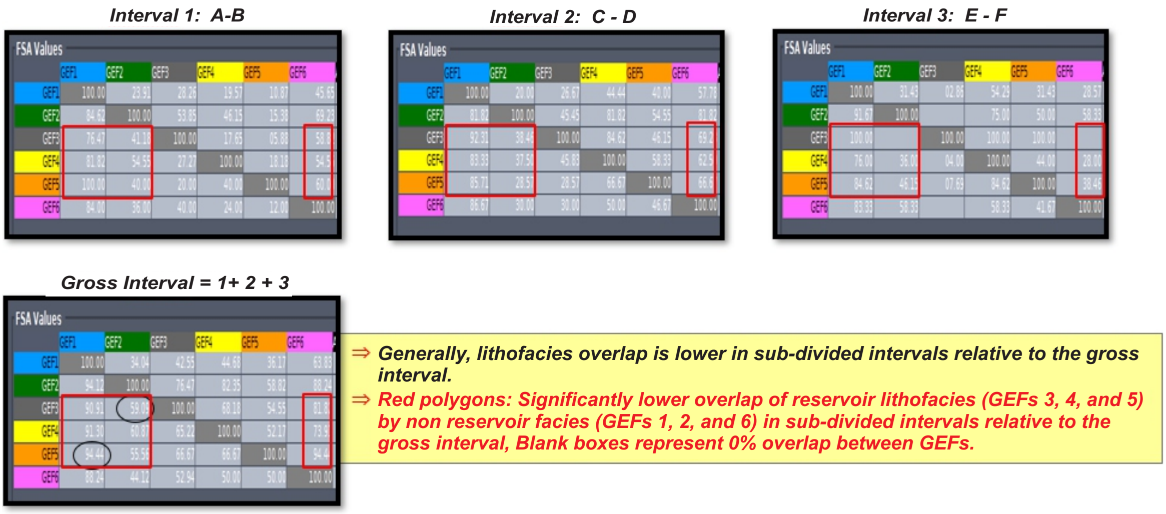

Figure 12: Quantitative comparison of overlaps (%) in GEFs between decoupled intervals (1, 2, and 3) and gross logged interval using Statistical Facies Superposition Analysis (SFSA). Overlaps of GEFs in decoupled intervals are lower: Note the significantly lower overlaps between reservoir lithofacies (GEFs 3, 4, and 5) and non-reservoir lithofacies (e.g., GEFs 1, 2, and 6) thus reducing uncertainties in reservoir/non-reservoir discrimination.

in rock physics behavior) may sometimes be merged to guarantee the stability of lithofacies operators or PDFs. The results of lithofacies/GEFs merging for one of the decoupled intervals (Interval 2) into mega GEFs (MGEFs) is presented in Figure 13. Though not presented in this paper, similar merging exercises in intervals 1 and 3 produced similar combinations of GEFs into MGEFs 1, 2, and 3.

The merging resulted in three MGEFs (1, 2, and 3). Ellipses represent GEF clustering intensity. Though not presented in this paper, similar merging exercises in intervals 1 and 3 produced the same combination of GEFs into MGEFs 1, 2, and 3. Note that data points are more than those in Figure xx due to increase in number of inverted extracted at wells to eliminate statistical bias.

Probability Density Functions of merged GEFs/Lithofacies and Facies Probability Cubes

Comparisons of operators or probability density functions for each lithofacies built from discrete set of points of merged GEFs (i.e., MGEF 1, 2, and 3) from IP versus Vp/Vs cross-plots for both the entire logged interval and one of the decoupled intervals (Interval 2) demonstrate the advantage of the decoupling scheme (Figure 14). In seismic reservoir characterization, the quality of a lithofacies characterization exercise can be determined from the degree of overlaps in PDFs. The PDFs for Interval 2 from the decoupled scheme showed reduced MGEF overlaps. For instance, the MGEF1 PDF from the entire logged interval exhibits some probabilities

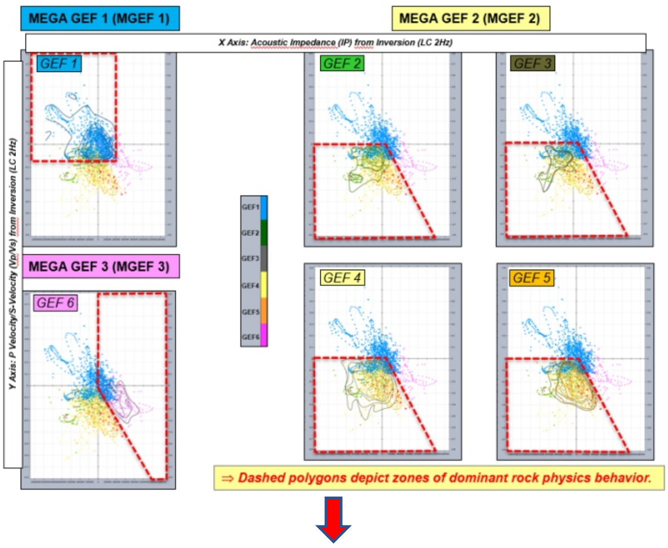

Figure 13: Merging of GEFs into mega GEFs in Interval 2 (R12; C – D; Figures 3 and 12) based on similarities in rock physics behavior.

of occurrence (%) in the southern two quadrants (Figure 14) which are not consistent with the rock physics behavior of shales in the study area (Figure 13). Though not presented in this paper, reduced MGEF overlaps were also observed in the PDFs for intervals 1 and 3 using the decoupling scheme.

Further value of adding the decoupling scheme to the conventional lithofacies characterization workflow was observed in the probability cube of each of the merged lithofacies/GEFs in 3D seismic space that was deduced after application of the PDFs to the full OBN seismic volume based on a convolution process. One important QC approach to the checking of the quality of a lithofacies characterization exercise is the prediction quality of lithofacies probability cubes at training wells and cross validation at one or two wells that are not part of the characterization workflow (i.e., blind wells). A complementary approach is a similar check of prediction quality using areal (2D or map) attribute extractions of sedimentary systems or architectural elements (AEs). Figure 15 highlights the first approach for the merged and 3 using the decoupling scheme. Though not presented in this paper, a similar robustness was observed in intervals 1 (R12) and 3 (R24) using the decoupling scheme.

Note the robust facies prediction at the blind well (DF-6) and well DF-8 (one of the training wells used in the lithofacies characterization). Areal disposition of the channel is also well constrained by the probability cube. Colors represent the probabilities of occurrence for MGEF2. A similar robustness was observed in turbidite channels in intervals 1 (R12) and 3 (R24) using the decoupling scheme.

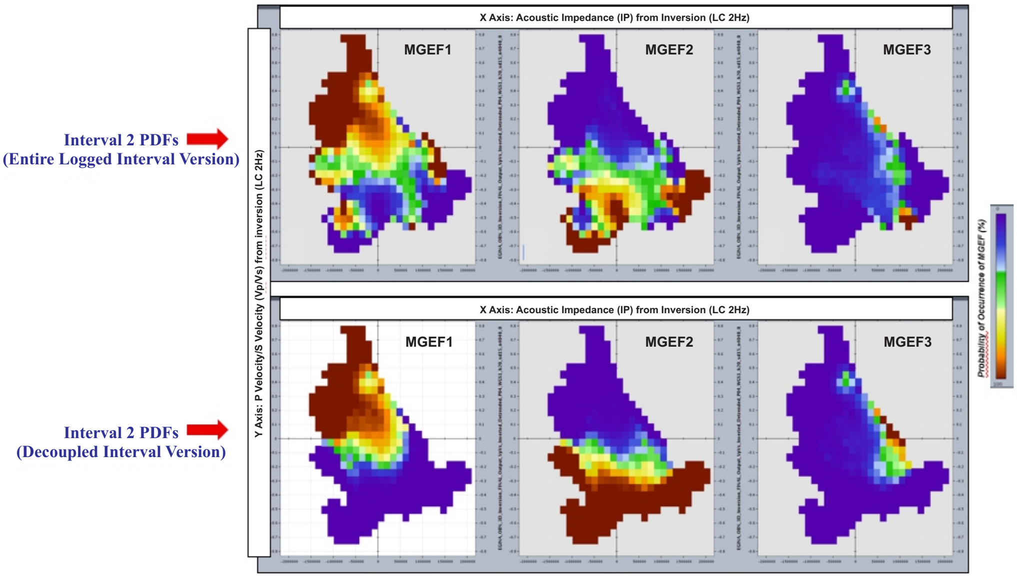

Figure 14: Evidence of robustness of decoupling scheme based on the comparison of PDFs for merged GEFs for Interval 2 as deduced using the entire logged interval (i.e., top three cross plots) and decoupled interval 2 (i.e., bottom three cross plots), respectively. Colors represent the probabilities of each merged GEF (MGEF) or lithofacies in the cross-plot space. A similar robustness was observed in PDFs for intervals 1 and 3 using the decoupling scheme.

GEF2 (i.e., MGEF2) in the study area, with the probability cube of MGEF2 of the decoupled interval 2 showing robust facies prediction/calibration with the upscaled GEF log at the well that was chosen as the blind well in our workflow (DF-6; see Figure 3 for location of well). On the other hand, 2D average in layer attribute of probability of occurrence (%) of merged GEF2 (MGEF2) in one of the turbidite channels in interval 2 (R18) using decoupling scheme is presented in Figure 16. Generally, the QCs point to very good calibration at the two wells (i.e., blind well DF-6 and training well DF-8) and excellent discrimination of MGEF2 (i.e., reservoir lithofacies) from the background or encasing non-reservoir facies (MGEFs 1 and/or 3). Though not presented in this paper due to space constraints, a similar robustness was observed in the quality of lithofacies prediction of the MGEF probability cubes for intervals 1

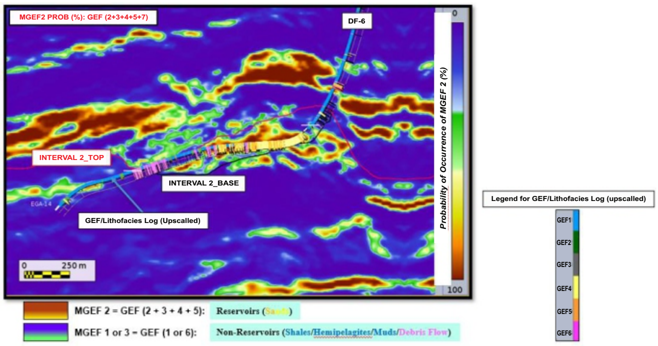

Figure 15: Random line through blind well (DF-6) showing robust facies prediction exhibited by merged GEF2 (MGEF2) probability cube for interval 2 (R18) using decoupling scheme. Colors represent the probabilities of occurrence for MGEF2. Location of the blind well is shown in Figures xx and xx.

CONCLUSIONS

We applied a reservoir (interval) decoupling scheme to Middle to Late Miocene turbidite sands and shales in the Delta Field in the Niger Delta to reduce classification

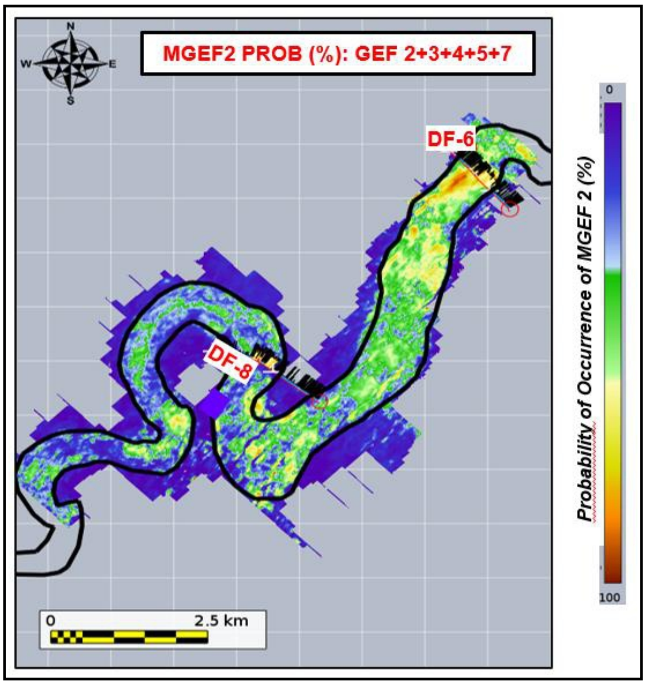

Figure 16: 2D average in layer attribute of probability of occurrence (%) of merged GEF2 (MGEF2) in one of the turbidite channels in interval 2 (R18) using decoupling scheme.

biases and uncertainties. The approach is qualitative, not computationally intensive, and does not require assumptions. It involved using multi-well rock physics analysis at seismic scale to identify statistical lithofacies populations within a lithofacies framework consisting of seven grouped electrofacies (GEFs), that exhibit significant overlaps in rock physics properties across the gross logged interval in the field. Based on facies overlap sensitivities in rock physics space using inverted IP and Vp/Vs attributes from Ocean Bottom Nodes (OBN) seismic data extracted at training wells, the vertical sequence was divided into three separate intervals consisting of lithofacies/GEFs with seismically important rock physics variations. Probability density functions (PDFs) and facies probability cubes from the decoupling approach showed better discrimination and correlations at wells when compared to those produced without the decoupling approach. Cross validation at blind wells indicated that the decoupled facies cubes are also more predictive based on excellent correspondence with well results. Reservoir modeling, well planning, and 4D seismic monitoring using the facies probability cubes from the decoupling scheme are ongoing with preliminary results indicating improved predictions of sand presence, reservoir properties (e.g., net to gross, porosities, et cetera) at wells. These improved predictions are expected to reduce uncertainties in the use of the lithofacies probability cubes as probabilistic indicators of reservoir and non-reservoir facies within the 3D reservoir grid, thus adding value to the overall reservoir management in the oil field. In our view, our decoupling approach would be useful in other turbidite fields where significant overlaps in rock physics behavior among lithofacies in different stratigraphic intervals are observed.

REFERENCES CITED

Amoyedo, S., E. Tawile, S. Pou-Palome, P. Kakaire, O. Olagundoye, J. Mascomere, and E. Owah (2020): Full wave and down-going elastic inversion of deep water OBN seismic data, example from the Niger Delta. Conference Proceedings, First EAGE Conference on Seismic Inversion, Oct 2020, Volume 2020, p.1 – 5.

Avseth, P., T. Mukerji, and G. Mavko, (2014): Quantitative seismic interpretation, applying rock physics tools to reduce interpretation risk: Cambridge University Press.

Chakraborty, S., E. L'Heureux, K. Hartman, Q. Li, I. Ahmed, C. Joy, and S. Michell (2017): Thunder Horse Ocean-Bottom Nodes acquisition design. SEG International Exposition and 87th Annual Meeting Extended Abstract, 226-230.

Ekweozor, C. M., and E. M. Daukoru, (1994): Northern delta depobelt portion of the Akata-Agbada petroleum system, Niger Delta, Nigeria, in, L. B. Magoon, and W. G. Dow, eds., The petroleum system, from source to trap: AAPG Memoir, 60, 599-614.

Hunt, L., S. Reynolds, S. Hadley, and J. Downton (2012): Quantitative Interpretation Part I: Method. CSEG Recorder.

Klett, T. R., T. S. Ahlbrandt, J. W. Schmoker, and J. L. Dolton (1997): Ranking of the world's oil and gas provinces by known petroleum volumes, U.S. Geological Survey Open-File Report, 97-463.

Michelena, R. J., K. S. Godbey, and P. E. Rodrigues (2010): Facies probabilities from multidimensional cross plots of seismic attributes. 2010 SEG Technical Meeting Denver Program Expanded Abstracts, 1377-1381.

Oliveira, L., F. Pimentel, M. Peiro, P. Amaral, and J. Christovan (2018): A seismic reservoir characterization and porosity estimation workflow to support geological model update: Pre-salt reservoir case study, Brazil. First Break 36(9), 75-85.

Pendrel, J. V., H. J. Schouten, R. Bornard (2017): Identifying and Mapping Facies from Petrophysics to Geophysics. GeoConvention, 1-5.

Reijers, T. J. A., S. W. Petters, and C. S. Nwajide (1997): The Niger delta basin, in R.C. Selley, ed., African basins, Sedimentary basin of the world 3: Elsevier Science, 151-172.

Short, K. C., and A. J. Stäuble (1965): Outline of geology of Niger delta: American Association of Petroleum Geologists Bulletin, 51, 761-779.

Singh, S. K., R. Tandon, P.K. Chaudhuri, A. Bhardwaj (2019): Geo-statistical Inversion for thin Reservoir Delineation & Sub-surface Uncertainty Estimation: A case study. GEOPIC, ONGC, Dehradun-248001, 1-7.: PETROTECH-2019 Conference. https://www.researchgate.net/publication/337894316.

Tawile, E., S. Amoyedo, O. Olagundoye, L. Kaucsar, and P. Kakaire (2020): Seismic-scale reservoir facies characterization using elastic inversion of OBN dataset, how to get past limitations from using only wells with elastic logs acquisition, 38th NAPE International Conference Expanded Abstract, Lagos, Nigeria.

Tuttle, M. L. W., R. R. Charpentier, and M. E. Brownfield (1999), The Niger Delta petroleum system, Niger Delta Province, Nigeria, Cameroon, and Equatorial Guinea, Africa: U.S. Geological Survey Open-File Report, 99-50-H.

Weber, K. J., and E. M. Daukoru (1975): Petroleum geology of the Niger delta, Proceedings of the Ninth World Petroleum Congress, 2: Applied Science Publishers, 210-221.

Weber, K. J. (1987): Hydrocarbon distribution patterns in Nigerian growth fault structures controlled by structural style and stratigraphy: Journal of Petroleum Science and Engineering, 1, 91-104.